Transparent Metamaterials for Multispectral Camouflage with Thermal Management

Namkyu Lee[a], Joon-Soo Lim[b], Injoong Chang[b], Donghwi Lee[c], Hyung Hee Cho[b]*

a. IBI-4, Forschungszentrum Jülich GmbH, 52425 Jülich, Germany

b. Department of Mechanical Engineering, Yonsei University, 50 Yonsei-ro, Seodaemun-gu, Seoul 03722, Korea

c. Department of Mechanical Engineering, University of Wisconsin–Madison, 1500 Engineering Drive, Madison, WI 53706, United States

* Corresponding author

Tel.: +82 2 2123 2828

Fax: +82 2 312 2159

E-mail: hhcho@yonsei.ac.kr

Abstract

Artificial camouflage surfaces, such as metamaterials, that interact with the electromagnetic (EM) wave represent an emerging field in which performance breakthroughs are occurring. In particular, the visible and infrared (IR) waves are of interest, because these waves are desirable for energy, military and space applications. However, needs of additional actuations, eccentric properties for a specific situation and complicated fabrications, with only a few reports to date, show that multispectral (visible and IR) camouflage surfaces are still challenging issues. Herein, we realize transparent metamaterials (TMM) as visible-IR camouflage surfaces. TMM achieves an average transmissivity of 0.44 in the visible regime. It also reduces the blackbody IR signature by 64% over 3-5 μm and 75% over 8-14 μm and dissipates 2200% more energy in the undetected band of 5-8 μm compared to an Au surface used for IR camouflage. These findings advance multispectral manipulation and expand energy applications in visible-IR waves.

Keywords:

Transparent metamaterials; Camouflage; Multispectral metamaterials; Transparent emitter; Energy dissipation;

1. Introduction

Camouflage is an instinctive behavior among animals that adapts their appearance to the surrounding environment, protecting the animals from external threats [1]. For example, chameleons and cephalopods change their color to blend into the background, making the animals difficult to observe [2]. Artificial camouflage surfaces, which manipulate the electromagnetic (EM) wave in the visible [3], infrared [4] and microwave [5,6], have recently emerged. The reason for increased interest is that artificial camouflage surfaces promise performance characteristics beyond the reach of existing materials and composites. Many researchers have investigated 'metamaterials' as artificial camouflage surfaces, as metamaterials realize designed EM properties including negative [7] and high [8] refractive index, optical switch [9] and selective emission [10,11].

Multispectral control surfaces covering both visible (380 - 740 nm) and IR (740 nm - 15 μm) waves, however, have been a few studied. Multispectral control surfaces for visible and IR waves are especially desirable for energy [12], military [13] and space applications [14]. For satisfying the mutual requirements of visible and IR camouflages, the surfaces should have visible transparency and IR selective emission simultaneously. For a visible camouflage, several creatures have presented their visible camouflage as a transparency such as glasswing butterflies [15] and glass frogs [16]. Even if they cannot hide perfectly contrary to a negative index surface [7], the transparency can provide the camouflage effectively which realized the state-of-the art fabrication. For IR camouflage [17–23], depending on the atmospheric window which is a transmitted band of IR wave in 3-5, 8-14 μm [24], IR camouflage surfaces is designed of lowering the emissivity in the detected (3-5, 8-14 μm) and undetected band (5-8 μm), because the molecules in air absorb IR waves of 5-8 μm. Thus, in the detected band (3-5, 8-14 μm), the camouflage surfaces reduce their signature by lower emissivity. In order to maintain thermal stability caused by lowering the energy dissipation, the increase of emissivity in the undetected band is necessary[25].

Up to date, there have been electro-thermochromic materials[26], conducting polymers[27], or mechanical actuations[28], which required the additional actuation for changing their properties, eccentric EM properties for a specific situation and complicated fabrications. For example, the unit cell size of metamaterials differs depending on the targeted wave, which the size is about 10 nm in the visible wave and about 1 mm for microwaves [29]; this wide range of sizes is difficult to fabricate onto the same surface. Additionally, EM properties of artificial camouflage surfaces are difficult to satisfy the various spectral waves, simultaneously. For example, conventional emitters consisting of metal-dielectric-metal (MDM) structures for IR camouflage [18–20] have high reflectivity in the visible wave preventing the use of camouflage pattern backside of emitters. Otherwise, some emitters that use transparent materials have been developed for broadband absorption [30,31] in the IR regime. Based on the circuit analysis, it is hard to get a selective emission in the IR regime because the transparent electrode has a higher electrical resistivity than the metal which induces the higher emissivity presented in Fig. S1. Thus, having properties of both visible transparency and IR selective emission simultaneously are challenging issues for artificial multispectral camouflage surfaces.

Herein, transparent metamaterials (TMM) are developed that offers both visible and IR camouflage simultaneously. For visible camouflage, a transparent material is used in creatures such as glasswing butterflies [15] and glass frogs [16]. For IR camouflage, selective emission is chosen, which reducing IR signature in the detected band (3-5, 8-14 μm), and dissipating the reduced signature through the undetected band (5-8 μm) [17–19] simultaneously, because the reduced emitting energy can cause the thermal instability [25] of target as we unwanted. Using a quartz and ITO wafer with an Au pattern, we reduce the impedance of structure for a selective emission in Fig. 1(a). The qualitative camouflage performance in the visible and IR waves is evaluated using cameras, and quantitative spectral measurements are taken of the transmissivity in the visible light and the emissivity in the IR wave, respectively. Ultimately, the TMM for achieving a multispectral visible-IR camouflage surface is demonstrated.

2. Research details

2.1. Geometry and fabrication methods

We applied a conventional metal-dielectric-metal (MDM) structure, as the basic structure of our TMM in Fig. 1(a). The TMM consists of four parts: substrate (quartz), total reflector (ITO), dielectric layer (Si_3N_4) and metal disks (Au). Quartz wafer is widely used as a substrate for micro-nano fabrication due to its visible transparency. In general, MDM structures use highly electrical conductive materials for the metal part because, as shown by a circuit analysis [6,32], the effective impedance of the structure is a function of the wavelength. However, conventional metals reflect visible and IR waves completely, preventing the desired visible transparency. Thus, we chose ITO as a total reflector which consumes large area at the bottom of MDM structure. The thickness of ITO is 400 nm, which reduces the electrical resistivity as much as possible to maintain the visible transparency. In case of metal disks, based on the circuit analysis, the lower equivalent impedance is important to maintain the selective emission even though the ITO reflector is used. When the blocked area ratio is small enough to penetrate the visible light, it is possible to maintain the visible transparency. It means that Au as metal disks can be used for decreasing the equivalent impedance. The thickness of Au metal disk is 100 nm with an adhesive layer (Ti) of 10 nm. Ti is a layer for improved adhesion on Si_3N_4, and does not affect the EM behavior, as shown in previous work [8]. The pitch is 3 μm, a disk diameter of 0.89 μm. As a dielectric layer, Si_3N_4 with a thickness of 100 nm is chosen because it has transparency and high permittivity in IR regime, similar to ZnS, which is widely used for IR camouflage material.

For the TMM, we prepared the quartz wafer substrate by rinsing and cleaning by sonication in acetone (5 min). Piranha solution (H_2SO_4:H_2O_2 = 3:1) was used to remove organic matter on the surface. A 400 nm layer of Ito was deposited on the prepared quartz wafer using batch sputter (ULDiS-4540SV, Korea Advanced Nano Fab Center) to reduce the resistance. Then, we deposited a 150 nm layer of silicon nitride (Si_3N_4) as a dielectric

layer, using PECVD (Plasma Therm 790 Series). On top, 100 nm Au disks were deposited by electron beam Evaporator (ULVAC) with adhesive layer of Titanium (10 nm). Using a spin coater (3000 rpm, 30 sec), we coated photoresist (AZ5214E) onto the prepared Au-Si_3N_4-ITO. By using an EVG Aligner (KIST, micro-nano fabrication center), we achieved sub-micron patterns by controlling the exposure time. We developed the pattern using MIF-300, observing the status of the pattern after 25-35 seconds. Using the oxford etcher, we etched the exposed gold, then removed the photoresist using plasma asher (100W, 5 min). Figure 1(b) shows the fabricated structures of TMMs.

2.2. Simulations

The transparent selective emitter was designed using the commercial solver, COMSOL Multiphysics v.5.2a, as a simulation tool. The simulated geometry consisted of four parts: the medium (air), a reflector (ITO), a dielectric layer (Si_3N_4) and metal disks (Au). Planar EM wavefronts at the two ports were assumed, using periodic boundary conditions for the side walls. We adopted the Drude-Lorentz dispersion model for analyzing the electromagnetic behaviors of ITO[30] (ε_r = 3.9, plasma frequency = 0.46 PHz, damping constant = 28.7 THz) and Au[33] (plasma frequency = 2.06 PHz, damping constant = 13.34 THz). The relative permittivity of the dielectric layer was applied following reference [34], while that of the air held the same as in vacuum ($\varepsilon_r = \mu_r = 1$). The finite element size was restricted to less than 500 nm, which was selected after a mesh independent test (Supplementary Information, Figure S2). After simulating the electromagnetic behavior, we derived the emissivity from the absorptivity because of Kirchhoff's law [35] and the following procedure. At the ports, we gathered the scattering parameters (S_{11}, S_{21}) [36] which resulted from the electromagnetic behaviors of a unit cell. S_{11} was the signal ratio of the incident and reflected wave which corresponded to the reflection coefficient, while S_{21} was the signal ratio of the incident and transmitted wave, which corresponded to the transmission coefficient. Based on Kirchhoff's law [35] and the scattering parameters [36], we deduce

the absorptivity (emissivity) as follows: $\alpha = 1 - \rho - \tau = 1 - |S_{11}|^2 - |S_{21}|^2$, where absorptivity is α, reflectivity is ρ, and transmissivity is τ, respectively.

2.3. Measurement of infrared emissivity

To measure the spectral emissivity, we used Fourier transform infrared spectroscopy (FT-IR, Bruker Corp.). The beam splitter was KBr for making phase difference, and the measurement wavelength range was from 1.3 μm to 27 μm. We measured the reflectivity of the emitter (Bruker A513) based on Kirchhoff's law [35] and using the following equation: $\varepsilon(\lambda) = \alpha(\lambda) = 1 - \rho(\lambda)$, where emissivity is ε, absorptivity is α, reflectivity is ρ and wavelength is λ, respectively. Due to a metal ground as shown in Fig. 1(a), we determined the transmissivity as zero. The signal ratio between the reference and sample signals was used to calculate the reflectivity of the sample as following equation: $\rho(\lambda) = S_{sample}(\lambda,T) / S_{reference}(\lambda,T)$, where the reflected signal is S and the temperature is T, respectively. During the measurement, we assumed that the temperature remained unchanged. The sample size was 1.3 cm x 1.3 cm, and the reference surface was Au with a thickness of 200 nm.

2.4. Measurement of visible transmissivity

A UV-Vis-NIR spectrophotometer (Cary 5000 UV-Vis-NIR) was used to measure transmissivity in the 175-3300 nm range. The main principle of spectrophotometer is used for the Beer-Lambert law. Defining the incident radiation as I_0 and the transmitted radiation as I, the transmittance is calculated as follows:

$$\tau = I/I_0$$

The reference material for incident radiation was ambient air, which was assumed to have 100% transmittance.

2.5. Thermographic and visible measurement

For observing the manipulated infrared radiation, thermographic images were measured by an IR camera (A655sc, FLIR Systems, Wilsonville, OR, US). The actual temperature of the specimen was controlled by the hotplate and set as 37°C to mimic the skin temperature of a human being. The processed emissivity of IR camera was taken as 0.95 as a default for comparing the differences in infrared radiation from different specimens. Visible images were measured by a 12 MP dual pixel camera with 1.4 μm pitch and an f/1.7 optically stabilized lens. It shows the visible camouflage based on a transparency of TMM in a visible regime. The detailed experimental set-up is available in the Supplementary information (Section 2.4).

3. Results and Discussions

3.1. Transparent metamaterials for simultaneous visible and infrared camouflage

For the transparent metamaterials, it is important to consider the material properties having a visible transparency and a selective emission in IR regime. In optics, metallic materials represent particles that hinder the path of EM waves inside the material [37]. Similarly, conducting polymers or ceramics having visible transparency can act as a metal ground in a selective emitter. For this reason, we chose ITO as a metal ground for the MDM structure, because it has electrical conductivity and visible transparency. The dielectric layer was chosen as silicon nitride, which has a visible transparency[38]. Au was chosen as a metal disk in order to reduce the electrical resistance of the MDM structure by considering the circuit analysis in Fig. S1. In general, metal disks act the same as ground materials[17–19]. However, ITO as a metal disk prohibits IR selective emission, because the high resistance of ITO induces high impedance over the width of the IR wave, which causes a wavelength independent emissivity in Fig. S1. Thus, we attempted to reduce the resistance by substituting the metal disk material, even though it required the sacrifice of some amount of transmittance in the visible light. As shown in Fig. S4, when we substituted Au for ITO, the TMM acquired IR selective emission. Additionally, the surface area blocked by the Au disks (diameter = 0.89 μm) was about 10% (pitch = 3 μm), which is transparent enough for visible camouflage. To observe the multispectral control provided by this TMM, we visualized the visible and IR graphics shown in Figs. 1(c) and (d). As desired, the symbol underneath the TMM is recognizable in Fig. 1(c). In Fig. 1(d), although the background and the TMM had the same temperature, the apparent temperature expressed as the IR signature is lower at the TMM. Based on the radiative heat flux equation[35], $q''=\varepsilon\sigma T^4$, where the emissivity is ε, the Boltzmann constant is σ, and the temperature is T, the lower apparent temperature expresses the lower radiative heat flux of the IR signature. At the default emissivity of 0.95 for the IR detector in Fig. S2, when the IR detector reports lower temperature, the radiative heat flux of the IR signature is also lower than the background level. It shows that the TMM can

manipulate the IR signature by manipulating that of surface emissivity. Therefore, these figures provide qualitative results for multispectral camouflage in the visible and infrared waves. To establish an understanding of the underlying principles of the TMM, the following sections analyze the optical behavior.

3.2. Optical characteristics of transparent metamaterials in the visible and infrared waves

In the field of atmospheric transmissivity, there are detected and undetected bands because the atmospheric molecules hinder the detection of infrared light through absorption. In general, 3-5 μm and 8-14 μm are detected bands, which are the blue-shaded areas in Fig. 2(a), and 5-8 μm is an undetected band, which has almost zero transmissivity. Depending on the target's temperature distribution, common IR detectors match their operating band to the detected bands, so for IR camouflage, IR is reduced in the 3-5 μm of hot parts and 8-14 μm of cold parts [39]. The reason is that radiative energy is a function of temperature and wavelength. When the target temperature increases, the peak wavelength of maximum radiative energy from the target decreases based on Wien's displacement law [35]. Moreover, because of the energy balance equation, we consider the energy dissipation of reduced infrared signature energy with regard to the thermal stability of the TMM [17,18]. Figure 2(a) shows that the TMM realizes selective emission in the undetected band and reduced emissivity in the detected band, making it suitable for IR camouflage performance.

To analyze the TMM in IR wave, we consider the plasmonic behavior, which is divided among localized and non-localized plasmons [40,41]. Through the validated simulation with experiment in Fig. S4(b), we reveal electromagnetic behaviors related to the occurrence of resonance. The localized plasmonic behavior, caused by EM confinement due to interactions within the structure, is dependent on the disk diameter, while the non-localized plasmonic behavior, caused by the intrinsic EM properties, is dependent on the pitch. Figures 2(b) and (c) present the simulated results as the disk diameter and pitch were changed, respectively. In Fig. 2(b), around 3.5 μm, there is a weak resonance indicating non-plasmonic behavior of the TMM. In comparison to diameter results, in Fig. 2(c), a strong resonance occurs around 6 μm, showing that the selective emission of the TMM for IR camouflage depends on localized plasmonic behavior, which can be controlled by changing the pitch. To visualize the localized plasmonic behavior, we simulate the magnetic field around the TMM, as shown in Fig. 2(d). Strong magnetic fields occur inside the TMM, which means that the TMM uses the same

principle for selective emission. However, the TMM exhibits different current directions in the metal ground and the disk parts. When the ground and disk consist of the same material, the current vector points in the same direction (0,1,0) under an exciting EM wave. Here, the current vectors is changed in the opposite direction compared to conventional emitters [18]. We may infer that the different resistivity in the ground and disk induces the opposing current directions. Additionally, it is desirable for the IR camouflage material to behave independent of the incident angle because IR detectors can be located at various angles with respect to the target. Figure 2(e) shows the spectral emissivity as a function of the incident angle. The figure demonstrates that the TMM can operate in the range of 0 - 60°, covering about 67% of the incident direction, which is sufficient coverage.

We also measured the visible transmissivity of the TMM. Figure 3(a) compares the spectral transmissivity of quartz with an ITO layer (400 nm) to that of the TMM, showing that the TMM has lower transmissivity. We analyze systematically the effect of the deposited layer. In general, quartz wafers with ITO exhibit visible transparency larger than 0.9, but in this work, the ITO thickness was greater than in other studies [42], leading to decreased visible transmissivity. Moreover, to understand the difference between quartz with an ITO layer and the TMM, we consider the blocking surface area and optical scattering. Due to the resistance of ITO, gold was chosen for the metal disk, but gold hinders the transmission of visible light through the structure. The surface area blocked by metal disks is 8.8%, leading to a maximum possible visible transmissivity of 0.69 based on the average ITO transmittivity of 0.76 in Fig. 3(a). In addition, the structure thickness is similar in scale to visible wavelengths, leading to Mie scattering [37]. Based on the measurements in Fig. 3(a), the TMM has 0.44 average transmissivity in the visible light (400-700 nm). We judge this transmissivity to be sufficient for a visible camouflage. To examine the visible transparency qualitatively, we compare the printed picture shown in Fig. 3(b) through air and the TMM, and confirm that the TMM has sufficient transparency.

3.3. Evaluation of visible-IR camouflage of transparent metamaterials

We evaluate the visible and IR camouflage performance of the TMM in comparison to a quartz wafer and a conventional emitter. In the case of visible transparency, the visible transmissivity is enough to express the camouflage performance. In the case of the IR camouflage, there are two ways to explain the IR camouflage performance. On the one hand, the direct measurement of radiation temperature represents the actual camouflage performance in detected bands [17,20]. On the other hand, the calculation of emissivity energy in the IR regime is utilized to evaluate the ideal camouflage performance [18,19]. In this study, we assess both to demonstrate the camouflage performance.

The quartz wafer provides high visible transmissivity and high IR emissivity, while the conventional emitter provides low visible transmissivity and IR selective emissivity. On a hot plate, we compared visible and IR graphics, using the experimental set-up described in Fig. S2. Figures 4(a) and (b) present the qualitative visible-IR camouflage performance. As shown in Fig. 4(a), the TMM and quartz wafer have visible transparency, while the conventional emitter obscuring the visible light from the backside of pattern. In a quantitative evaluation shown in Fig. 4(c), the averaged visible (400-700 nm) transmissivity of quartz, the TMM, and the conventional emitter was 0.95, 0.48, and 0.0008, respectively. The results demonstrate that the TMM obtains the visible camouflage capabilities because of its visible transparency.

Figure 4(b) compares IR images of the specimens. The hot plate temperature was maintained at 37°C, corresponding to actual specimen temperatures. The average apparent temperature of quartz was 35.7°C, while that of the TMM was 27.8°C, which was lower than that of quartz wafer and similar to that of conventional emitter, 25.4°C. These results follow because, in 8-14 μm, the spectral emissivity of the TMM is slightly higher than that of the conventional emitter, as shown in Fig. 4(d). However, the apparent temperature difference between the quartz and TMM (7.9°C) was much larger than the difference between the transparent and

conventional emitters (2.4°C), indicating that the TMM has similar IR camouflage performance to a conventional emitter.

Furthermore, to quantify the amount of signature reduction and energy dissipation for IR camouflage, we integrated the spectral irradiance in the detected bands (3-5 μm and 8-14 μm) and the undetected band (5-8 μm), respectively. The spectral irradiance is calculated by following equation [35]:

$$E_{b\lambda}(\lambda, T) = \frac{2\pi h c_0^2}{\lambda^5 \left[\exp[\frac{hc_0/k}{\lambda T} - 1]\right]} \quad (1)$$

where $E_{b\lambda}$, λ, h, c_0, k and T are spectral blackbody emissive power, the wavelength, Planck's constant, the speed of light in a vacuum, Boltzmann constant and the temperature, respectively. Figure 5 shows the spectral irradiance of a 310 K blackbody (human body temperature), the TMM, and a gold surface. The blackbody surface represents ideal energy dissipation, while the Au surface provides ideal IR signature reduction and an IR camouflage surface [13]. In terms of signature reduction, we compare the radiative flux between the blackbody and the TMM in the detected bands (3-5 μm and 8-14 μm). To evaluate the radiative flux, we use the discretized equation based on the spectral emissivity by FT-IR as follows [17–19]:

$$E_{\lambda_1-\lambda_2}(T) = \int_{\lambda_1}^{\lambda_2} \varepsilon(\lambda, T)\, E_{b\lambda}(\lambda, T)\, d\lambda \cong \sum \varepsilon(\lambda, T)\, E_{b\lambda}(\lambda, T)\Delta\lambda \quad (2)$$

where λ_1, λ_2 and ε are the shortest and longest wavelength of the band, and spectral emissivity, respectively. Over 3-5 μm and 8-14 μm bands, respectively, the radiative flux of the blackbody is 8.3 W/m^2 and 203.3 W/m^2, respectively. The TMM is 3.0 W/m^2 and 51.7 W/m^2, which are 36% and 25% of the blackbody's radiative flux. These values demonstrate that the TMM can significantly reduce the IR signature. To study the energy dissipation that accompanies the infrared signature reduction, we compare the radiative fluxes of gold and the TMM over the undetected band of 5-8 μm. The radiative flux of the gold surface is 1.68 W/m^2 and that of the TMM is 37.0 W/m^2, which is an 2200% increase in dissipated energy of signature reduction. In summary,

these results show that the TMM provides satisfactory visible camouflage performance and IR camouflage performance via IR signature reduction in the detected bands and shifted energy dissipation toward the undetected band.

4. Conclusion

In summary, we investigated an TMM for simultaneous visible-IR camouflage based on multispectral control. Starting from a metamaterial with an MDM structure, we substituted the ground material with ITO, which offers visible transparency and electrical conductivity that reflects IR waves, yielding selective emission in IR wave. To verify the design concept, we analyzed the visible and IR optical behavior of the fabricated emitter through qualitative analysis (visible and thermographic images) and quantitative analysis (UV-vis-NIR and FT-IR spectrometer). These results confirm that the TMM achieves 36% and 25% of the IR signature of a blackbody, which expresses the maximum IR signature of object, in the detected bands of 3-5 μm and 8-14 μm, respectively. Simultaneously, the TMM increases the energy dissipation of an Au surface, which is ideal surface for IR signature reduction, by 2200% in the undetected band of 5-8 μm.

Typically, selective emitters are only used for single-band control in the visible light (photovoltaic), infrared wave (thermophotovoltaics, camouflage), and microwave (camouflage). However, the TMM developed here realizes multispectral control over a wavelength range spanning two orders of magnitude, simultaneously. The used structure size having the order of 1 μm is facile to fabricate except for microscopic structures being the order of 10 nm. Furthermore, based on the parametric studies presented here, the TMM can target different applications by straightforward modification of the compositional materials, layer thicknesses, and pitches. If the advanced transparent electrode whose electrical conductivity is similar to the metal is developed, we would expect the spectral emissivity of TMM with maintaining the visible transparency can be identical with the conventional IR camouflage material. These findings give a stepping stone for advanced multispectral manipulation in the visible-IR waves, and also potential routes for expanded energy applications using visible-IR waves.

Author Information

Corresponding Author

*E-mail: hhcho@yonsei.ac.kr

Author contributions

N. L., and H. H. C. designed and performed the experiment. N. L., J.-S. L. and D. L. fabricated the samples. N. L. and J.-S. L. performed the optical characterizations by the FT-IR facility. N. L. and I. C. conducted the numerical simulation for the optical characterization. All the authors analyzed the data. N. L. and H. H. C. wrote and supervise the manuscript.

Acknowledgements

This work was supported by the Human Resources Development program (No. 20204030200110) of the Korea Institute of Energy Technology Evaluation and Planning (KETEP), grant funded by the Korea government Ministry of Trade, Industry and Energy and also was supported by Basic Science Research Program through the National Research Foundation of Korea(NRF) funded by the Ministry of Education(2019R1A6A3A03033316)

References

[1] I.C. Cuthill, W.L. Allen, K. Arbuckle, B. Caspers, G. Chaplin, M.E. Hauber, G.E. Hill, N.G. Jablonski, C.D. Jiggins, A. Kelber, J. Mappes, J. Marshall, R. Merrill, D. Osorio, R. Prum, N.W. Roberts, A. Roulin, H.M. Rowland, T.N. Sherratt, J. Skelhorn, M.P. Speed, M. Stevens, M.C. Stoddard, D. Stuart-Fox, L. Talas, E. Tibbetts, T. Caro, The biology of color, Science 357 (2017) eaan0221.

[2] Z. Li, P. Liu, X. Ji, J. Gong, Y. Hu, W. Wu, X. Wang, H.-Q. Peng, R.T.K. Kwok, J.W.Y. Lam, J. Lu, B.Z. Tang, Bioinspired Simultaneous Changes in Fluorescence Color, Brightness, and Shape of Hydrogels Enabled by AIEgens, Adv. Mater. 32 (2020) e1906493.

[3] B. Zheng, R. Zhu, L. Jing, Y. Yang, L. Shen, H. Wang, Z. Wang, X. Zhang, X. Liu, E. Li, H. Chen, 3D Visible-Light Invisibility Cloak, Adv. Sci. 5 (2018) 1800056.

[4] Z.J. Coppens, J.G. Valentine, Spatial and Temporal Modulation of Thermal Emission, Adv. Mater. 29 (2017) 1701275.

[5] N.I. Landy, S. Sajuyigbe, J.J. Mock, D.R. Smith, W.J. Padilla, Perfect metamaterial absorber, Phys. Rev. Lett. 100 (2008) 207402.

[6] F. Costa, A. Monorchio, G. Manara, Analysis and Design of Ultra Thin Electromagnetic Absorbers Comprising Resistively Loaded High Impedance Surfaces, IEEE Trans. Antenn. Propag. 58 (2010) 1551–1558.

[7] V.G. Veselago, The electrodynamics of substances with simultaneously negative values of ε and μ, Sov. Phys. Usp. 10 (1968) 509–514.

[8] M. Choi, S.H. Lee, Y. Kim, S.B. Kang, J. Shin, M.H. Kwak, K.-Y. Kang, Y.-H. Lee, N. Park, B. Min, A terahertz metamaterial with unnaturally high refractive index, Nature 470 (2011) 369–373.

[9] Y. Hu, J. You, M. Tong, X. Zheng, Z. Xu, X. Cheng, T. Jiang, Pump-Color Selective Control of Ultrafast All-Optical Switching Dynamics in Metaphotonic Devices, Adv. Sci. 7 (2020) 2000799.

[10] C.M. Watts, X. Liu, W.J. Padilla, Metamaterial electromagnetic wave absorbers, Adv. Mater. 24 (2012) OP98-120, OP181.

[11] D. Hasan, C. Lee, Hybrid Metamaterial Absorber Platform for Sensing of CO2 Gas at Mid-IR, Adv. Sci. 5 (2018) 1700581.

[12] Q. Liao, P. Zhang, H. Yao, H. Cheng, C. Li, L. Qu, Reduced Graphene Oxide–Based Spectrally Selective Absorber with an Extremely Low Thermal Emittance and High Solar Absorptance, Adv. Sci. 7 (2020) 1903125.

[13] H. Tian, H.-T. Liu, H.-F. Cheng, A thin radar-infrared stealth-compatible structure: Design, fabrication, and characterization, Chin. Phys. B 23 (2014) 025201.

[14] D.U. Yildirim, A. Ghobadi, M.C. Soydan, O. Atesal, A. Toprak, M.D. Caliskan, E. Ozbay, Disordered and Densely Packed ITO Nanorods as an Excellent Lithography-Free Optical Solar Reflector Metasurface, ACS Photon. 6 (2019) 1812–1822.

[15] M. Arias, J. Mappes, C. Desbois, S. Gordon, M. McClure, M. Elias, O. Nokelainen, D. Gomez, Transparency reduces predator detection in mimetic clearwing butterflies, Funct. Ecol. 33 (2019) 1110–1119.

[16] J.B. Barnett, C. Michalis, H.M. Anderson, B.L. McEwen, J. Yeager, J.N. Pruitt, N.E. Scott-Samuel, I.C. Cuthill, Imperfect transparency and camouflage in glass frogs, Prog. Natl. Acad. Sci. U.S.A. 117 (2020) 12885–12890.

[17] T. Kim, J.-Y. Bae, N. Lee, H.H. Cho, Hierarchical Metamaterials for Multispectral Camouflage of Infrared and Microwaves, Adv. Funct. Mater. 29 (2019) 1807319.

[18] N. Lee, T. Kim, J.-S. Lim, I. Chang, H.H. Cho, Metamaterial-Selective Emitter for Maximizing Infrared Camouflage Performance with Energy Dissipation, ACS Appl. Mater. Interf. 11 (2019) 21250–21257.

[19] N. Lee, B. Yoon, T. Kim, J.-Y. Bae, J.-S. Lim, I. Chang, H.H. Cho, Multiple Resonance Metamaterial Emitter for Deception of Infrared Emission with Enhanced Energy Dissipation, ACS Appl. Mater. Interf. 12 (2020) 8862–8869.

[20] M. Pan, Y. Huang, Q. Li, H. Luo, H. Zhu, S. Kaur, M. Qiu, Multi-band middle-infrared-compatible camouflage with thermal management via simple photonic structures, Nano Energy 69 (2020) 104449.

[21] Ziquan Xu, Qiang Li, Kaikai Du, Shiwei Long, Yang Yang, Xun Cao, Hao Luo, Huanzheng Zhu, Pintu Ghosh, Weidong Shen, Min Qiu, Spatially Resolved Dynamically Reconfigurable Multilevel Control of Thermal Emission, Laser Photon. Rev. 14 (2020) 1900162.

[22] Y. Qu, Q. Li, L. Cai, M. Pan, P. Ghosh, K. Du, M. Qiu, Thermal camouflage based on the phase-changing material GST, Light Sci. Appl. 7 (2018) 26.

[23] H. Zhu, Q. Li, C. Zheng, Y. Hong, Z. Xu, H. Wang, W. Shen, S. Kaur, P. Ghosh, M. Qiu, High-temperature infrared camouflage with efficient thermal management, Light. Sci. Appl. 9 (2020) 60.

[24] D.C. Harris, Materials for Infrared Windows and Domes: Properties and Performance, SPIE, 1999.

[25] D.P. Sheehan, Infrared Cloaking, Stealth, and the Second Law of Thermodynamics, Entropy 14 (2012) 1915–1938.

[26] Y. Zhou, M. Layani, F.Y.C. Boey, I. Sokolov, S. Magdassi, Y. Long, Electro-Thermochromic Devices Composed of Self-Assembled Transparent Electrodes and Hydrogels, Adv. Mater. Technol. 1 (2016) 1600069.

[27] P. Chandrasekhar, B.J. Zay, G.C. Birur, S. Rawal, E.A. Pierson, L. Kauder, T. Swanson, Large, Switchable Electrochromism in the Visible Through Far-Infrared in Conducting Polymer Devices, Adv. Funct. Mater. 12 (2002) 95–103.

[28] C. Xu, M. Colorado Escobar, A.A. Gorodetsky, Stretchable Cephalopod-Inspired Multimodal Camouflage Systems, Adv. Mater. 32 (2020) e1905717.

[29] N. Engheta, Circuits with light at nanoscales: optical nanocircuits inspired by metamaterials, Science 317 (2007) 1698–1702.

[30] G. Dayal, S. Anantha Ramakrishna, Broadband infrared metamaterial absorber with visible transparency using ITO as ground plane, Opt. Exp. OE 22 (2014) 15104–15110.

[31] Y. Huang, Mingbo Pu, Ping Gao, Zeyu Zhao, Xiong Li, Xiaoliang Ma, Xiangang Luo, Ultra-broadband large-scale infrared perfect absorber with optical transparency, Appl. Phys. Exp. 10 (2017) 112601.

[32] Y. R. Padooru, Alexander B. Yakovlev, Chandra S. R. Kaipa, Francisco Medina, Francisco Mesa, Circuit modeling of multiband high-impedance surface absorbers in the microwave regime, Phys. Rev. B 84 (2011) 35108.

[33] E. Hecht, Optics, Addison Wesley San Francisco, 2002.

[34] N. Liu, M. Mesch, T. Weiss, M. Hentschel, H. Giessen, Infrared perfect absorber and its application as plasmonic sensor, Nano Lett. 10 (2010) 2342–2348.

[35] J. Kischkat, S. Peters, B. Gruska, M. Semtsiv, M. Chashnikova, M. Klinkmüller, O. Fedosenko, S. Machulik, A. Aleksandrova, G. Monastyrskyi, Y. Flores, W.T. Masselink, Mid-infrared optical properties of thin films of aluminum oxide, titanium dioxide, silicon dioxide, aluminum nitride, and silicon nitride, Appl. Opt. 51 (2012) 6789–6798.

[36] Y. Cengel, Heat and mass transfer: fundamentals and applications, McGraw-Hill Higher Education, 2014.

[37] S.J. Orfanidis, Electromagnetic waves and antennas, 2002.

[38] H.R. Philipp, Optical properties of silicon nitride, J. Electrochem. Soc. 120 (1973) 295–300.

[39] T. Kim, H. Lee, J.-Y. Bae, T. Kim, J. Cha, D. Jung, H.H. Cho, Susceptibility of combat aircraft modeled as an anisotropic source of infrared radiation, IEEE Trans. Aerosp. Electron. Syst. 52 (2016) 2467–2476.

[40] T. A. Kelf, Y. Sugawara, R. M. Cole, J. J. Baumberg, M. E. Abdelsalam, S. Cintra, S. Mahajan, A. E. Russell, P. N. Bartlett, Localized and delocalized plasmons in metallic nanovoids, Phys. Rev. B 74 (2006) 245415.

[41] T.D. Dao, K. Chen, S. Ishii, A. Ohi, T. Nabatame, M. Kitajima, T. Nagao, Infrared Perfect Absorbers Fabricated by Colloidal Mask Etching of Al–Al2O3–Al Trilayers, ACS Photonics 2 (2015) 964–970.

[42] M. Wang, A. Barnabé, Y. Thimont, J. Wang, Y. He, Q. Liu, X. Zhong, G. Dong, J. Yang, X. Diao, Optimized properties of innovative ElectroChromic Device using ITO / Ag / ITO electrodes, Electrochimica Acta 301 (2019) 200–208.

Supplementary Information

Transparent Metamaterials for Multispectral Camouflage with Thermal Management

Namkyu Lee[a,b], Joon-Soo Lim[b], Injoong Chang[b], Donghwi Lee[c], Hyung Hee Cho[b]*

a. IBI-4, Forschungszentrum Jülich GmbH, 52425 Jülich, Germany

b. Department of Mechanical Engineering, Yonsei University, 50 Yonsei-ro, Seodaemun-gu, Seoul 03722, Korea

c. Department of Mechanical Engineering, University of Wisconsin–Madison, 1500 Engineering Drive, Madison, WI 53706, United States

* Corresponding author

Tel.: +82 2 2123 2828

Fax: +82 2 312 2159

E-mail: hhcho@yonsei.ac.kr

1. Circuit analysis for the optical behavior of transparent metamaterials

Circuit analysis is widely used for understanding and designing structures in the microwave regime, particularly for frequency selective surfaces (FSS)[1]. Additionally, this analysis is applicable over the entire wavelength as the literature shows, with some deviations[2–4]. Thus, we utilized circuit analysis for the preliminary design of our transparent metamaterials (TMM).

Circuit analysis usually analyzes the AC electrical behavior, because phase differences and impedance mismatch induce reflection losses[1]. Electromagnetic (EM) waves have analogous AC characteristics. Figure S1(a) depicts a transmission line as a circuit for analyzing FSS structures, and the output signal. The circuit consists of three parts: the input signal, the FSS structure, and the output signal. We only consider the electrical impedance characteristics, which determine the reflection, absorption, and transmission at the interfacial surface between different mediums. Since TMM has a metal ground after the disk pattern, the transmission was set to zero for the analysis. Additionally, we analyze the absorptivity of the FSS because Kirchhoff's law shows that the absorptivity is the same as the emissivity.

At the input, EM waves penetrate the air, which has impedance = 377 Ohms[5]. Then, the EM wave meets the metal-dielectric-metal (MDM) structure, whose equivalent impedance determines the absorptivity. The periodic pattern can be converted into the equivalent impedance by combining the resistance, inductance, and capacitance as shown in Fig. S1(b) and the following equations:

$$Z_{FSS} = R + j\omega L - j\left(\frac{1}{\omega C}\right) \tag{1}$$

$$R \approx R_s(D^2/L^2), \; L \approx \frac{Z_0 D}{2c\pi}\ln\left(\csc\left(\frac{\pi w}{2D}\right)\right), \; C \approx \frac{2D\varepsilon_l^{qs}}{cZ_0\pi}\ln\left(\csc\left(\frac{\pi w}{2D}\right)\right)$$

where electrical resistance is R, the pattern pitch is D, the disk size is L, the speed of light in vacuum is c, the equivalent permittivity of the medium ε_l^{qs}, and the gap between disks is w, respectively. The reflected wave from metal ground is considered by the following impedance equation:

$$Z_d \approx R_{metal\ ground} + j\frac{Z_0}{\sqrt{\varepsilon_r}}\left(tan\left(k_0 d\sqrt{\varepsilon_r}\right)\right) \quad (2)$$

where j, ε_r, d and k_0 are the imaginary part, the relative permittivity, the thickness of the dielectric layer, and angular wave number, respectively. Based on these relations, we determine the absorption of the FSS as the following equation:

$$\alpha = \varepsilon = 1 - \gamma = |r|^2 = \left|\frac{Z_{eq} - Z_{air}}{Z_{eq} + Z_{air}}\right|^2 \quad (3)$$

where absorptivity is α, emissivity is ε, reflectivity is γ, the reflection coefficient is r and the impedance of the medium is Z_{eq}, respectively. Figure S1(c) shows the dependence of the absorptivity on the equivalent impedance; high absorptivities above 0.9, were obtained from 200 Ohm to 720 Ohm. It is desirable to match the value of the equivalent impedance around 377 Ohm at the specific target wavelength for IR selective emission.

Based on Eqs. (1)-(3), we can calculate the equivalent impedance. With these relations, we determine the qualitative effect of the metal ground on spectral emissivity. We assume that the disk diameter and pitch of the pattern are 1.5 μm and 3 μm, respectively; that the thickness of the dielectric layer is 150 nm with relative permittivity of 4.94 (at 6 μm)[6] and that the resistance of the pattern is 0.01 Ohm/sq, which is small enough to obtain IR selective emission in the IR wave. Figure S1(d) shows the effect of the resistance of the metal ground on the spectral emissivity in the IR wave. Increasing the resistance both widens the bandwidth of the selective emission, and increases the overall emissivity. The reasons for these effects relate to the dominant factors in

the equivalent impedance calculation. The resistance is not a function of frequency, contrary to the inductance and capacitance in Eq. (1), meaning that the resistance term reduces the effects of gap, pitch, and size on the selective emission and acts like a lossy material in the microwave[2,3]. Therefore, it is desirable to reduce the effect of resistance for IR selective emission.

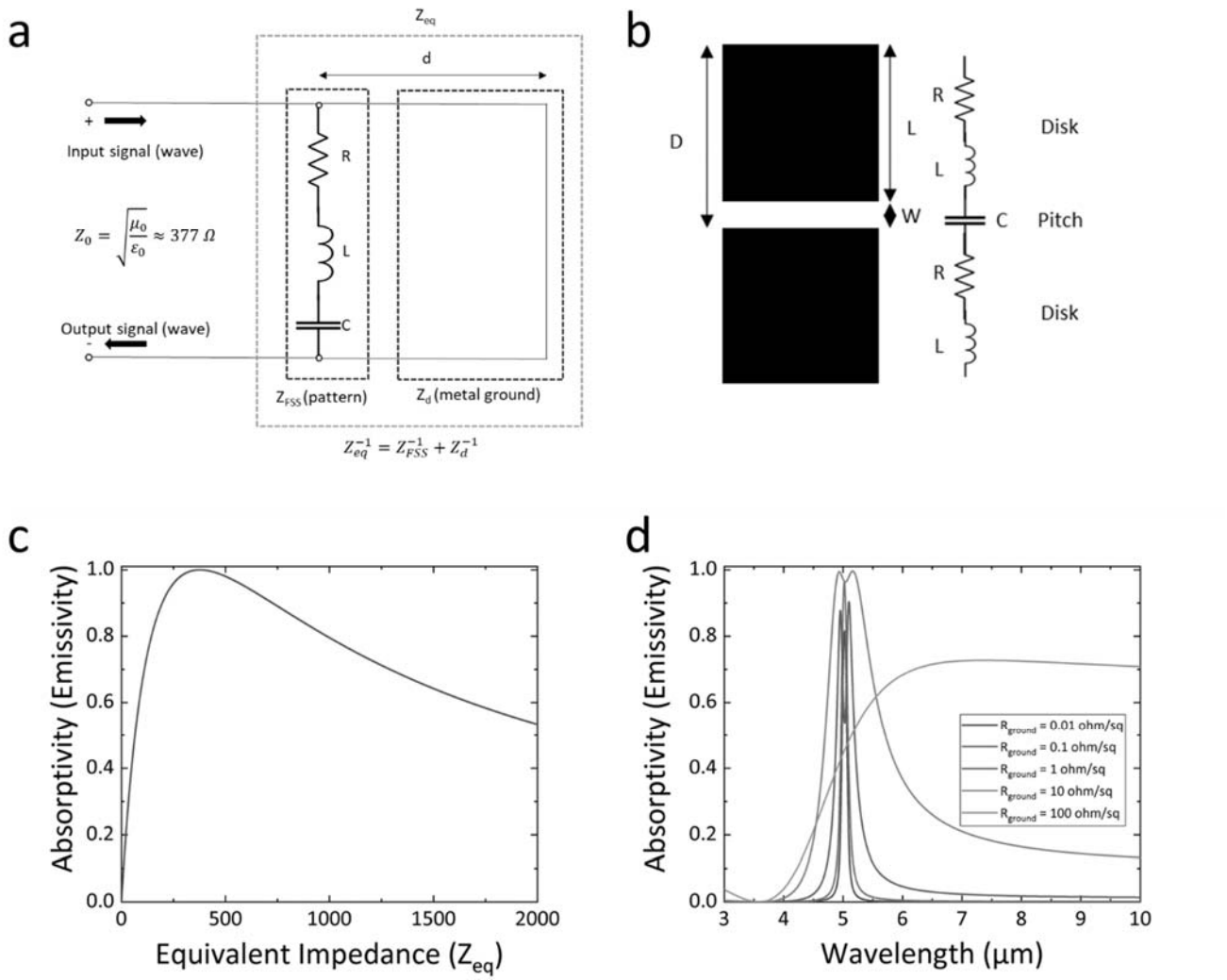

Figure S1. (a) Schematic of a transmission line as a circuit for analyzing the absorptivity (emissivity) of a frequency selective structure and (b) the geometrical conversion of a metal disk into a capacitance, inductance and a resistance. (c) Graph of absorptivity (emissivity) as a function of equivalent impedance. (d) Spectral emissivity of MDM structure as a function of the sheet resistance of the metal ground.

2. Qualitative visible and IR graphics evaluation of camouflage performance

Figure S2 shows the experimental set up of the qualitative evaluation of camouflage performance using visible IR graphics. As shown in Fig. S4, the transparent emitter, quartz wafer and conventional emitter specimens were placed on the paper with printed symbols above a hot plate whose temperature was 37°C. Before the experiment, we measured the actual temperature of quartz wafer with a K-type thermocouple, and the temperature of the quartz wafer was 35.8°C varying over the surface by up to 0.7°C during the experiment. Visible and IR cameras were installed above the specimens and captured similar fields of view for visible and IR graphical comparisons. The visible camera had a 12MP dual pixel sensor with 1.4-micron pixels and used an optically stabilized f/1.7 lens. The operating wavelength range of the IR camera was 8-14 μm. Graphical data processing was performed on a personal computer. For visible graphics, no post-processing was applied after data was downloaded from the camera. The IR image was converted into a temperature assuming a surface emissivity of 0.95, which is the default value of the post processing program used.

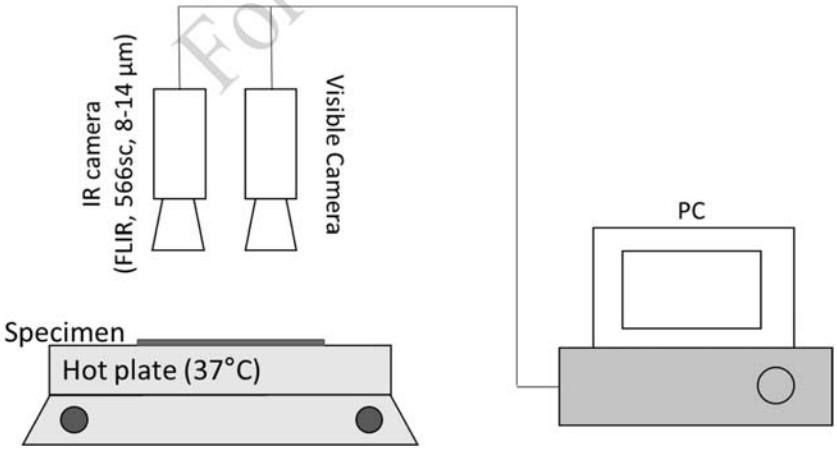

Figure S2. Schematic of the experimental set up for qualitative evaluation of visible and IR camouflage performance, using a hot plate with printed symbols on paper.

3. Grid independence test

Figure S3 shows the results of a grid independence test for our numerical simulations. In numerical simulations, the governing equation is discretized into finite elements, which means that the grid size affects the simulation results. For this reason, grid independence tests are performed to check the effect of the number of grids on the simulation results. As shown in Fig. S2, the numerical simulation is independent of the number of grids once the number of grids exceeds 6785. In this study, we choose 14099 grids, which corresponds to a maximum element size below 500 nm.

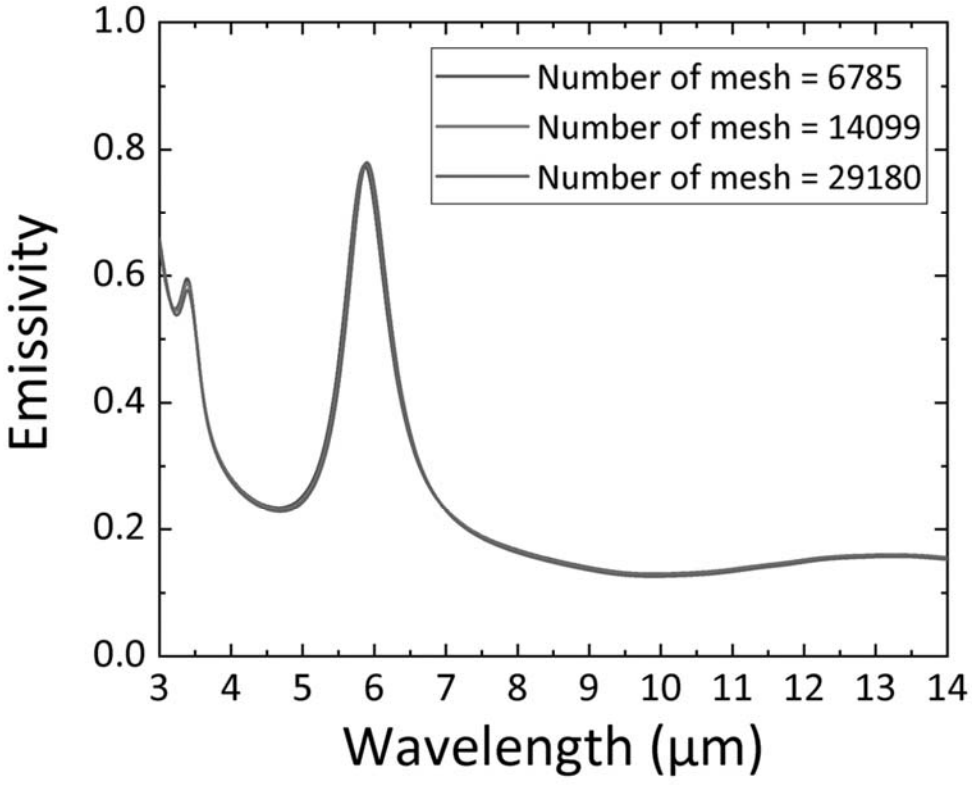

Figure S3. Graph of spectral emissivity as a function of the number of grids

4. Parametric study of transparent metamaterials

Figure S4 shows a parametric study of the effect of the thicknesses of the dielectric layer and the metal disk pattern of ITO and gold on the spectral emissivity of TMM. The thickness of the ITO ground plane is 400 nm, the diameter and pitch of the metal disks are 1 μm and 3 μm, respectively. Based on the circuit analysis (Supplementary Information, Section 1), the thickness of dielectric layer and the resistance of the metal ground and disk pattern critically affect the emissivity. For this reason, in designing TMM, we examined the effect of these factors on the spectral emissivity by simulation. Figure S4(a) shows the effect of the thickness of the patterned ITO disks and the effect of changing the disk material to Au. In case of ITO, selective emission does not occur because the impedance is large at the specific wavelength. However, when we change the material to metal (Gold) and decrease the resistance, selective emission appears at the specific wavelength, meaning that the change in material reveals the wavelength dependent impedance.

Figure S4(b) shows that increasing the thickness of dielectric layer increases the overall spectral emissivity. In general, increased thickness of the dielectric layer acts to increase the impedance, which is fitted to the air impedance (377 Ohm), and the impedance is a function of wavelength. Based on this numerical analysis, we chose the thickness of the dielectric layer to be 150 nm and the metal disk material to be Au (t = 100 nm). The red scattered data presented the experimental results showing a good agreement with simulation data. It meant that the simulation result can provide the electromagnetic behavior in the transparent metamaterials.

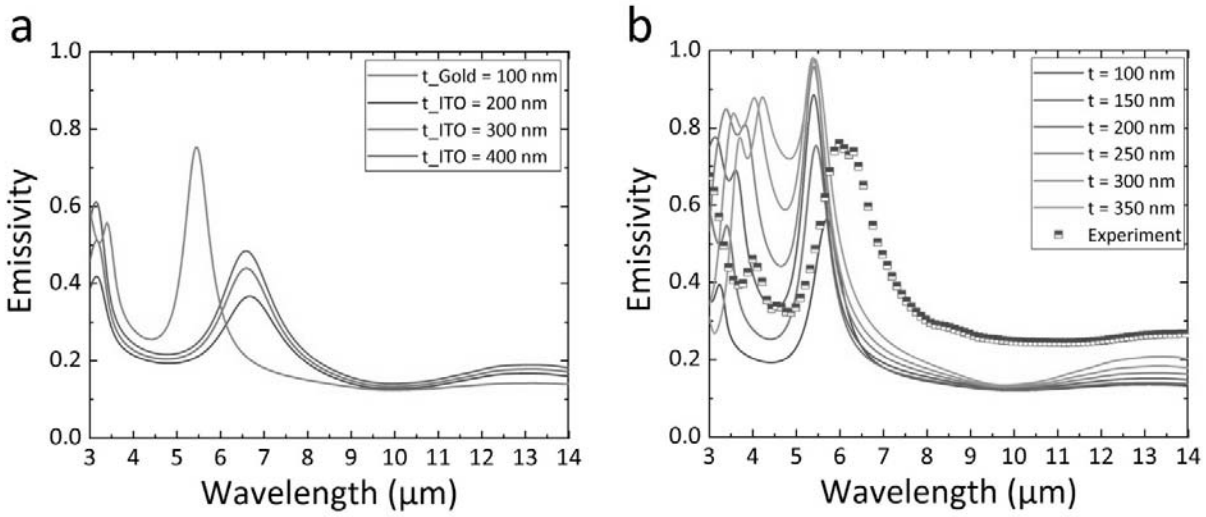

Figure S4. Parametric study of the spectral emissivity of TMM as a function of (a) the material and thickness of the metal disk and (b) the thickness of the dielectric layer. Additionally, the simulated results are validated with experimental data (red dot scattered data).

References

1 S. J. Orfanidis, Electromagnetic waves and antennas, 2002.

2 F. Costa, A. Monorchio and G. Manara, Analysis and Design of Ultra Thin Electromagnetic Absorbers Comprising Resistively Loaded High Impedance Surfaces, *IEEE Transactions on Antennas and Propagation*, 2010, **58**, 1551–1558.

3 Yashwanth R. Padooru, Alexander B. Yakovlev, Chandra S. R. Kaipa, Francisco Medina and Francisco Mesa, Circuit modeling of multiband high-impedance surface absorbers in the microwave regime, *Phys. Rev. B*, 2011, **84**, 35108.

4 N. Engheta, Circuits with light at nanoscales: optical nanocircuits inspired by metamaterials, *Science (New York, N.Y.)*, 2007, **317**, 1698–1702.

5 D. K. Cheng, Fundamentals of engineering electromagnetics, 1993.

6 J. Kischkat, S. Peters, B. Gruska, M. Semtsiv, M. Chashnikova, M. Klinkmüller, O. Fedosenko, S. Machulik, A. Aleksandrova, G. Monastyrskyi, Y. Flores and W. T. Masselink, Mid-infrared optical properties of thin films of aluminum oxide, titanium dioxide, silicon dioxide, aluminum nitride, and silicon nitride, *Applied optics*, 2012, **51**, 6789–6798.

Answers to the 1st Reviewer's Comments

We appreciate the significant efforts that the reviewer put into our paper to review. The reviewer raised comments about the manuscript. We will respond to those suggestions in the following statements. According to the reviewer's opinion, we changed the manuscript with notification by highlighting and attached a full list of changes.

(Comment #1)

The performance of the device in detected bands (3-5 μm and 8-14 μm) is not so excellent. The emissivity of the device in these bands is above 0.3. Is the high emissivity related to the character of ITO or the intrinsic absorption of Si_3N_4 in LWIR? Some discussions on reducing the emissivity in these bands are recommended?

(Answer)

The reviewer inquired the reason for higher emissivity in detected bands and further development to reduce the emissivity. To consider the material effect on the spectral emissivity, the authors simulate MDM structure depending on the material, such as indium tin oxide (ITO) and Au. Figure R1 shows the spectral emissivity depending on the material in metal parts.

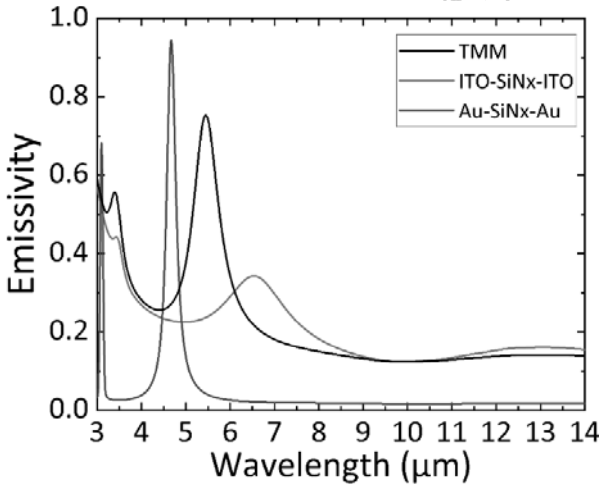

Figure R1. Simulated spectral emissivity of metal-dielectric-metal structure depending on the material in metal parts.

As shown in Fig. R1, we recognize the difference in spectral emissivity depending on the material. In the case of Au as metal parts, the emissivity in detected bands is low enough to hide the target, similar to the previous study. Conversely, in the case of ITO as metal parts, the emissivity in detected bands is 0.2, which value is similar to TMM suggested in this study. It means that ITO is the dominant impact on the spectral emissivity of TMM. For a further understanding, we described the circuit analysis in the IR regime in the supplementary information. Figure S1 (c) shows the relation between the equivalent impedance of metamaterial and medium.

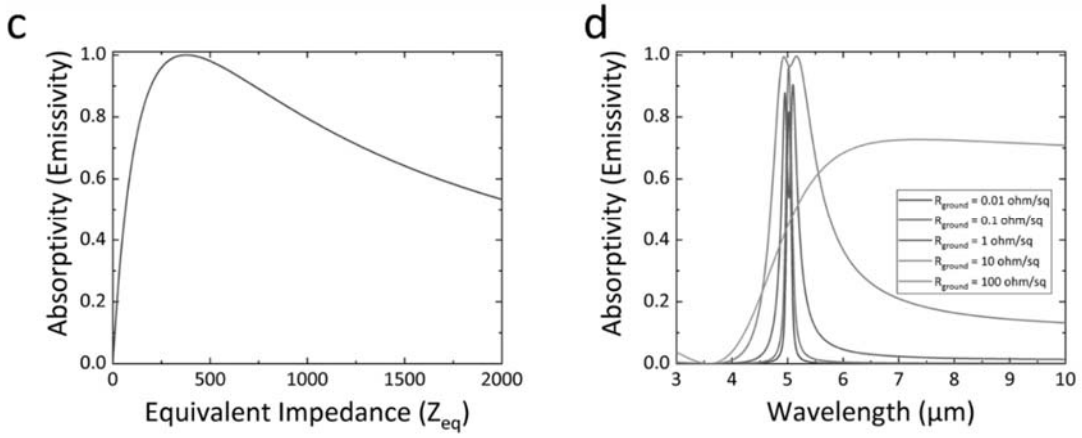

Figure S1. (c) Graph of absorptivity (emissivity) as a function of equivalent impedance. (d) Spectral emissivity of MDM structure as a function of the sheet resistance of the metal ground.

As shown in Fig. S1(c), we can understand that the emissivity is 1.0 at the equivalent impedance of 377 ohms. Moreover, the equivalent impedance above 377 ohms maintains the high emissivity. It means that the high resistance material leads to the high equivalent impedance, which induces the high emissivity. To check the effect of resistance, we calculate the emissivity with changes in metal ground resistance. As shown in Fig. S1(d), as the metal ground resistance increases, the overall emissivity also increases. Especially, when the metal ground resistance exceeds the certain value, the selective emission disappears. Since the electrical resistivity of ITO is 4-5 higher order of resistivity than the metal, we conclude that the higher emissivity happens in detected bands.

We also considered the contribution of Si_3N_4 to the spectral emissivity. In general, Si_3N_4 is opaque in the IR band, which means that the emissivity is almost 1. However, as materials become thin (O ~ 100 nm), it can be transparent as a Beer-Lambert law. To check this behavior, we calculate the transmissivity considered by the internal reflection. Figure R2 shows the transmissivity of Si_3N_4 with the wavelength in 3-14 μm.

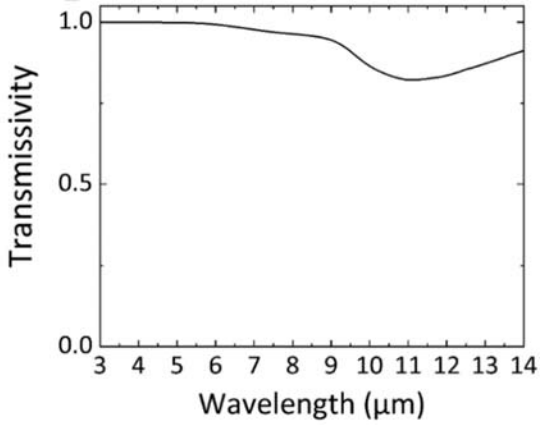

Figure R2. Calculated transmissivity of Si_3N_4 with the thickness of 100 nm used in this study.

As shown in Fig. R2, we understand that the transmissivity is high (> 0.8) except around 10 μm, caused by the lattice resonance interacting with the electromagnetic wave. If Si_3N_4 affects the spectral emissivity dominantly,

then the peak occurs about 10 μm as decreasing the transmissivity in Fig. R2. In Fig. R1, there is no peak around 10 μm. This result means that the Si_3N_4 has little impact on the spectral emissivity of TMM.

Based on these analyses, to realize a lower emissivity of TMM in detected bands, a novel transparent electrode having similar electrical conductivity to the metal is needed. ITO is one of the best materials having a visible transparency and low IR emissivity, which electrical conductivity is not enough to reduce the emissivity as much as the metal. Therefore, achieving the perfect visible-IR camouflage material needs the development of a transparent electrode. As the reviewer mentioned, we add and revise some explanations about the main reason for spectral emissivity. We also add the discussion written in this response as follow:

Revised and Added Sentences in Introduction (Page. 4)

"…Otherwise, some emitters that use transparent materials have been developed for broadband absorption [30,31] in the IR regime. Based on the circuit analysis, it is hard to get a selective emission in the IR regime because the transparent electrode has a higher electrical resistivity than the metal which induces the higher emissivity presented in Fig. S1. Thus, having properties of both visible transparency and IR selective emission simultaneously are challenging issues for artificial multispectral camouflage surfaces.…"

Revised and Added Sentences in Introduction (Page. 4)

"…Using a quartz and ITO wafer with an Au pattern, we reduce the impedance of structure for a selective emission in Fig. 1(a)..…"

Revised and Added Sentences in Research details (Page. 5)

"…Thus, we chose ITO as a total reflector which consumes large area at the bottom of MDM structure. The thickness of ITO is 400 nm, which reduces the electrical resistivity as much as possible to maintain the visible transparency. In case of metal disks, based on the circuit analysis, the lower equivalent impedance is important to maintain the selective emission even though the ITO reflector is used. When the blocked area ratio is small enough to penetrate the visible light, it is possible to maintain the visible transparency. It means that Au as metal disks can be used for decreasing the equivalent impedance. The thickness of Au metal disk is 100 nm with an adhesive layer (Ti) of 10 nm. Ti is a layer for improved adhesion on Si_3N_4, and does not affect the EM behavior, as shown in previous work[8]. The pitch is 3 μm, a disk diameter of 0.89 μm. As a dielectric layer, Si_3N_4 with a thickness of 100 nm is chosen because it has transparency and high permittivity in IR regime, similar to ZnS, which is widely used for IR camouflage material.…"

Added Sentences in Results (Page. 9)

"…For the transparent metamaterials, it is important to consider the material properties having visible transparency and a selective emission in IR regime. …"

Added Sentences in Conclusion (Page. 14)

"…If the advanced transparent electrode whose electrical conductivity is similar to the metal is developed, we would expect the spectral emissivity of TMM with maintaining the visible transparency can be identical with the conventional IR camouflage material. …"

(Comment #2)

Two methods have been proposed for evaluating the thermal camouflage with thermal management before. The first one is using an integrated factor for evaluating the camouflage performance based on the concept of energy balance (Eqs.[3-5] in Ref. [18] and Eq. 2 in Ref.[20]). The second one is direct measuring the radiation temperature with a fixed input heat source (Refs.[20, 23])). Some discussions on evaluating the thermal camouflage with thermal management of the proposed device are recommended.

(Answer)

The reviewer asked which evaluations suggested from the authors represented the camouflage performance, which are the calculation of radiative energy and a direct measure of radiation temperature from the target. The first concept is the radiative energy ratio between undetected and detected bands [Ref. N. Lee, et al., ACS Appl. Mater. Interf. **2019**, 11 (23), 21250-21257]. As we mentioned in the manuscript, the energy dissipation in undetected bands due to the reduced emissivity in detected bands was important for preventing the thermal instability of the system. Thus, we suggested evaluating the camouflage performance, including the reduced and enhanced radiative energy simultaneously. We thought the calculation of radiative energy representing the ideal camouflage performance of material in a radiative cooling or a camouflage performance without considering the background. The second measurement [Ref. M. Pan, et al., Nano Energy **2020**, 69, 104449; H. Zhu, et al., Light Sci. Appl. **2020**, 9, 60] is a direct observation on the radiation temperature with a fixed input heat source. It is one of the easiest ways to show the modified emissivity in the detected band of IR camera. It has a meaning of the magnitude of recognition in the real condition, which considers the difference between the target and background. In summary, the first factor is the performance factor in an ideal condition. The second factor is the operating factor that is close to the real condition. We, the authors, are thankful for this thoughtful comment and add some discussions in the manuscript as follow:

Added Sentences in Results 3.3 (Page. 14)

"…In the case of visible transparency, the visible transmissivity is enough to express the camouflage performance. In the case of the IR camouflage, there are two ways to explain the IR camouflage performance. On the one hand, the direct measurement of radiation temperature represents the actual camouflage performance in detected bands [17,20]. On the other hand, the calculation of emissivity energy in the IR regime is utilized to evaluate the ideal camouflage performance [18,19]. In this study, we assess both to demonstrate the camouflage performance.…"

(Comment #3)

Some abbreviations should be specified. For example, "TMM" in the abstract and "O~10nm", "O~1mm" in the introduction.

(Answer)

We, the authors, are thankful for your detailed comments. We revised and added some sentences as follows:

Revised Sentence in Abstract (Page. 2)

"…*Herein, we realize transparent metamaterials (TMM) as visible-IR camouflage surfaces*…."

Revised Sentence in Introduction (Page. 4)

"…For example, the unit cell size of metamaterials differs depending on the targeted wave, which the size is about 10 nm in the visible wave and about 1 mm for microwaves [29];…"

Revised Sentence in Conclusion (Page. 14)

"…The used structure size having the order of 1 μm is facile to fabricate except for microscopic structures being the order of 10 nm. …"

(Comment #4)

The colorbar of some figures should be modified. For example, it will be more convincing to substitute "H" and "C" in Fig. 1(d) with Max and Min.

(Answer)

The reviewer commented that it is better to indicate the temperature in Fig. 1(d) with Max and Min. The authors agreed to the reviewer's opinion because the temperature value is essential to convince the camouflage performance on the heated plate. Thus, we revised the figure as follow:

Revised Figure 1

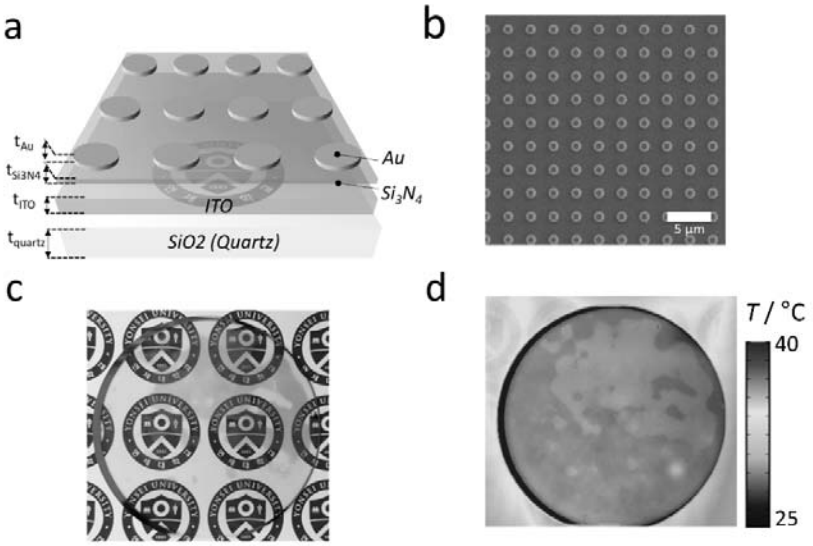

Figure 1. (a) Schematic of transparent metamaterials (TMM) structure, which consists of quartz (substrate), indium tin oxide (ITO) (metal ground), Si_3N_4 (dielectric layer) and Au/Ti (metal disks). (b) Scanning electron microscope (SEM) image of the fabricated TMM (disk diameter = 0.89 μm, pitch = 3 μm, t_{ITO} = 0.4 μm, t_{Si3N4} = 0.15 μm and $t_{Au/Ti}$ = 0.1/0.01 μm. (c) Visible images of the TMM. (d) IR thermograph of the TMM.

(Comment #5)

The page number for Ref.[21] is missing and it should be 1900162.

(Answer)

The reviewer commented on some typos in the manuscript, including the reference. We revised and added some typos in the manuscript as follows:

Revised References

[13] H. Tian, H.-T. Liu, H.-F. Cheng, A thin radar-infrared stealth-compatible structure: Design, fabrication, and characterization, Chin. Phys. B 23 (2014) 025201.

[21] Ziquan Xu, Qiang Li, Kaikai Du, Shiwei Long, Yang Yang, Xun Cao, Hao Luo, Huanzheng Zhu, Pintu Ghosh, Weidong Shen, Min Qiu, Spatially Resolved Dynamically Reconfigurable Multilevel Control of Thermal Emission, Laser Photon. Rev. 14 (2020) 1900162.

Answers to the 2nd Reviewer's Comments

We appreciate the significant efforts that the reviewer put into our paper to review. The reviewer raised a comment about the manuscript. We will respond to those suggestions in the following statements. According to the reviewer's opinion, we changed the manuscript with notification by highlighting and attached a full list of changes.

(Comment #1)

The emissivity near the wavelength of 3 μm is still high for the purpose of infrared stealth. Did the author consider the reason causing this result and the methods to avoid the high infrared emissivity?

(Answer)

The reviewer commented that the relative high emissivity of TMM in 3-5 μm is difficult for applying the camouflage material. We think that it is insufficient to explain IR camouflage contents in the manuscript. The emissive energy is dependent on the temperature and wavelength based on Stefan-Boltzmann's law as the following equation:

$$E_{b\lambda}(\lambda, T) = \frac{2\pi h c_0^2}{\lambda^5 \left[\exp[\frac{hc_0/k}{\lambda T} - 1]\right]} \quad (1)$$

Based on Eq. (1), as the temperature increases, the peak wavelength moves toward the shorter wavelength, Wien's displacement law. It means that the emissive energy from hot parts (> 600°C) emits through 3-5 μm and such energy from cold parts (<100°C) dissipates through 8-14 μm, which is the same procedure in the IR camouflage. Figure R3 shows the schematics of temperature distribution on the aircraft [Ref. T. Kim, et al., J. KIMST, Vol. 17, No. 6, pp. 764-772, 2014.]. As shown in Fig. R3, we recognize that the emissivity energy at the rear fuselage skin heated by engine/plume emits through 3-5 μm. The nose, canopy, intake and leading edges radiate through 8-14 μm caused by aerodynamic heating. In the case of 3-5 μm, the absolute IR intensity is so high that it is possible to avoid threats using the artificial hot source such as flair. However, In the case of 8-14 μm, since the IR seeker finds the intensity contrast between target and background, there is no way to evade threats. Thus, it is much more critical to reduce the IR signature in 8-14 μm than 3-5 μm [Ref. T. Kim et al., IEEE Trans. Aerosp. Electron. Sys., **2016** vol. 52, no. 5, pp. 2467-2476]. Thus, we have tried to lower the spectral emissivity in 8-14 μm at first.

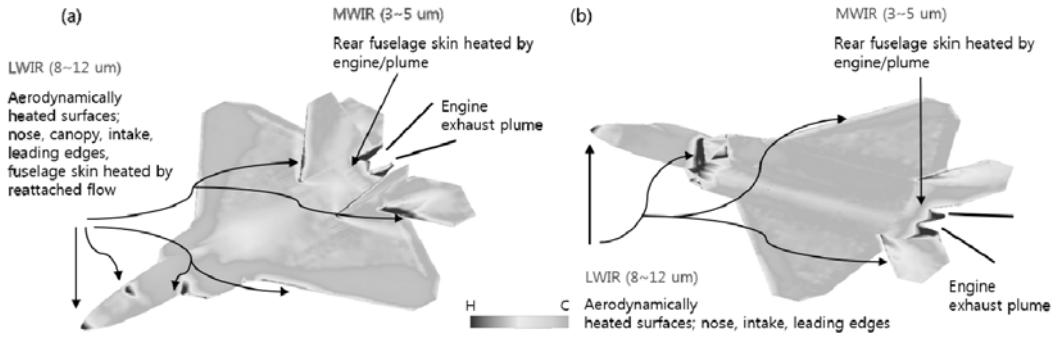

Figure R3. Schematic of temperature distribution on the aircraft calculated by the numerical simulation.

In IR seeker, they observe the total energy flux in detected bands. It means that some of the peak values are not dominant impact on the total emissivity energy. In TMM, although the emissivity around 3 μm is about 0.7, the averaged emissivity is 0.36 in 3-5 μm, which value is possible for hiding the signature to confuse the IR seeker as we think. Additionally, TMM has visible transparency, which makes enhanced survivability against external threats in visible regime.

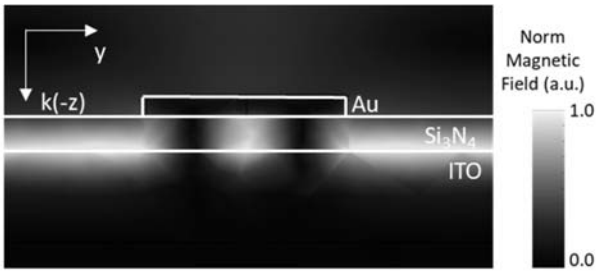

Figure R4. Magnetic field of TMM at 3 μm.

Moreover, the high peak below 3-4 μm is not easy to control because it is related to metal's intrinsic property. Figure R4 shows the magnetic field at the cross-section of the y-z plane. Different from Fig. 2(d), the magnetic field happens at the interface of Si_3N_4 and ITO. We think that the surface plasmonic behavior occurs and induces the emissivity at 3 μm. Unfortunately, the non-localized plasmonic behavior like the surface plasmonic behavior is not controlled by changing the geometrical factors because the intrinsic properties of dielectric material and metal originate its plasmonic behavior. It is also observed in the conventional MDM structure around 3 μm [Ref. N. Lee, et al., ACS Appl. Mater. Interf. **2019**, 11, 23, 21250–21257; N. Lee, et al., ACS Appl. Mater. Interf. **2020**, 12, 7, 8862–8869]. Thus, it is needed to develop the novel transparent electrode or find the material having a visible transparency and IR reflectivity simultaneously to solve this problem. Related to the discussion, we need to add sentences for general readers in 'International Journal of Heat and Mass Transfer' as follow:

Added Sentences in Results and Discussion (Page. 12)

"Depending on the target's temperature distribution, common IR detectors match their operating band to the detected bands, so for IR camouflage, IR is reduced in the 3-5 μm of hot parts and 8-14 μm of cold parts [39]. The reason is that radiative energy is a function of temperature and wavelength. When the target temperature increases, the peak wavelength of maximum radiative energy from the target decreases based on Wien's displacement law [35]."

(Comment #2)

For metamaterials with metal substrates, the average emissivity in the wavelengths of atmosphere windows can be below 10%. However, with the ITO substrate, this part of emissivity is relatively higher. Does the absorption of ITO in the infrared wavelength range lead to this?

(Answer)

The reviewer commented the higher emissivity of TMM compared to the conventional emitter composed of metals. We think that higher emissivity is due to the higher resistance of the material (ITO) than the metal. As we mentioned in the circuit analysis in the supplementary information, when the equivalent impedance of the material is

identical with the medium's impedance (377 ohms), the emissivity will be 1. Additionally, as shown in Fig. S1(c), the equivalent impedance above 377 ohms steadily maintains the higher emissivity. It means that the increase of resistance in metal parts induces the higher emissivity because the equivalent impedance is close to the air (377 ohms). In Fig. S1(d), the spectral emissivity is a function of the sheet resistance in the metal ground. We can understand that the higher sheet resistance leads to the higher emissivity and weakens the selective emission. Based on this result, we conclude that the higher resistance of ITO induces the higher emissivity in the IR regime compared to the conventional emitter.

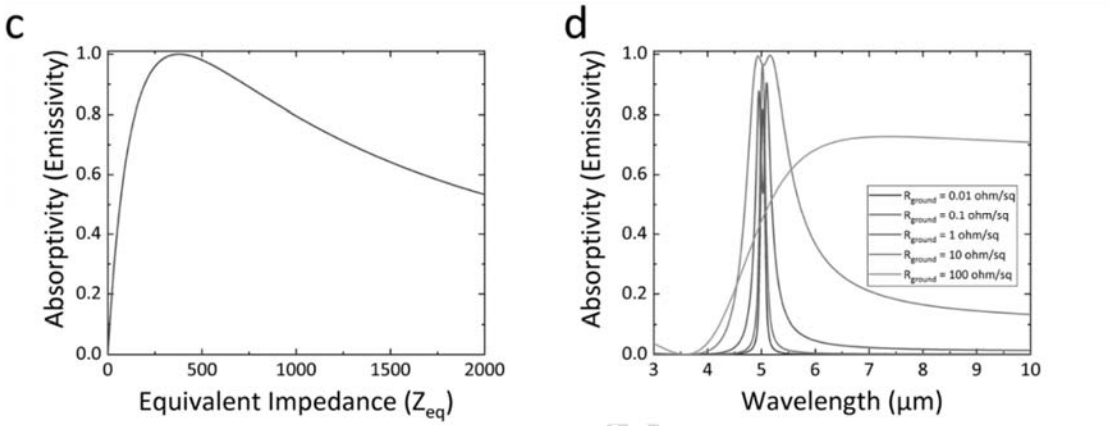

Figure S1. (c) Graph of absorptivity (emissivity) as a function of equivalent impedance. (d) Spectral emissivity of MDM structure as a function of the sheet resistance of the metal ground.

To check this hypothesis of the material effect on the spectral emissivity, we simulate MDM structure depending on the material such as indium tin oxide (ITO) and Au. Figure R1 shows the spectral emissivity depending on the material in metal parts.

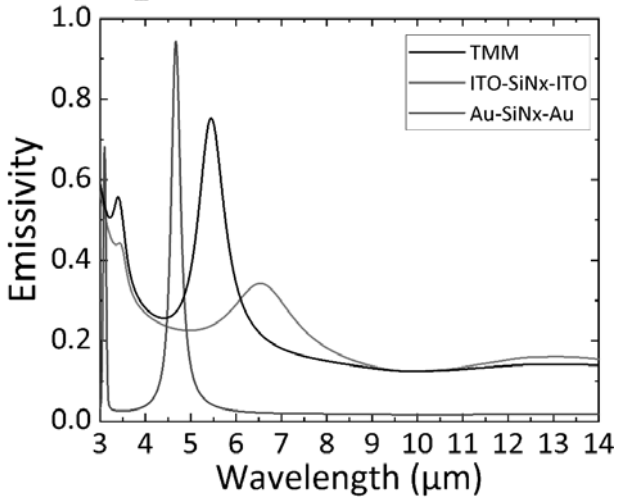

Figure R1. Spectral emissivity of metal-dielectric-metal structure depending on the material in metal parts.

As shown in Fig. R1, we understand the difference in spectral emissivity depending on the material. In the case of Au as metal parts, the emissivity in detected bands is low enough to hide the target, similar to the previous study. Conversely, in the case of ITO as metal parts, the emissivity in detected bands is 0.2, which value is close to TMM suggested in this study. Generally, the emissivity is related to the electrical conductivity of the material at a certain wavelength. The reason is that particles causing the electrical current interact with the electromagnetic wave and induce the material's reflectivity. Thus, we recognize high spectral emissivity in detected bands generated by the high resistance of ITO compared to the metal such as Au.

Based on these analyses, to realize a lower emissivity of TMM in detected bands, a novel transparent electrode having similar electrical conductivity to the metal is needed. ITO is one of the best materials with visible transparency and low IR emissivity, which electrical conductivity is not enough to reduce the emissivity as much as the metal. Therefore, the development of a transparent electrode is needed for achieving the perfect visible-IR camouflage material. As the reviewer mentioned, we add and revise some explanations about the main reason for spectral emissivity. We also add the discussion written in this response as follow:

Revised and Added Sentences in Introduction (Page. 4)

"…Using a quartz and ITO wafer with an Au pattern, we reduce the impedance of structure for a selective emission in Fig. 1(a). …"

Revised and Added Sentences in Research details (Page. 5)

"…Thus, we chose ITO as a total reflector which consumes large area at the bottom of MDM structure. The thickness of ITO is 400 nm, which reduces the electrical resistivity as much as possible to maintain the visible transparency. In case of metal disks, based on the circuit analysis, the lower equivalent impedance is important to maintain the selective emission even though the ITO reflector is used. When the blocked area ratio is small enough to penetrate the visible light, it is possible to maintain the visible transparency. It means that Au as metal disks can be used for decreasing the equivalent impedance. The thickness of Au metal disk is 100 nm with an adhesive layer (Ti) of 10 nm. Ti is a layer for improved adhesion on Si_3N_4, and does not affect the EM behavior, as shown in the previous work [8]. The pitch is 3 μm, a disk diameter of 0.89 μm. As a dielectric layer, Si_3N_4 with a thickness of 100 nm is chosen because it has transparency and high permittivity in IR regime, similar to ZnS, which is widely used for IR camouflage material.…"

(Comment #3)

What is the inner mechanism of enhanced transmittivity with quartz wafers?

(Answer)

In this study, we suggest TMM having the visible transparency and the IR camouflage performance simultaneously. To secure the electromagnetic (EM) wave's transparency, we choose the monotonical decrease of refractive index by increasing the wavelength, called a normal dispersion. Conversely, due to the resonance between the EM wave and atoms in the material, if the change of refractive index with the wavelength abruptly increases, the anomalous dispersion occurs, which causes the high absorption around the resonance regime. Since this behavior is related to material's intrinsic property, it is not easy to choose the appropriate material for realizing the transparency at a certain regime. By considering these characteristics, we choose the quartz wafer and ITO for visible transparency.

Additionally, the IR camouflage material is based on MDM structure. However, the metal reflector at the bottom of the MDM structure blocked the EM wave completely, which causes the visible recognition by threats. Thus, to substitute the metal reflector, we should understand the 'metallic behavior' of material in optics. As we know, the 'metallic behavior' happens due to the interaction between the material atoms and EM wave [Ref. E. Hecht, Optics, Addison Wesley San Francisco, 2002]. It means that the conductive material can act as the metal reflector of MDM structure. Since our objective is the visible transparency with IR camouflage performance, we judged that the transparent electrode such as ITO can be a metal reflector. Besides, we should perform lithographic procedures because the feature size is about 1 μm. It leads to the quartz wafer because it has visible transparency (>0.95) and low roughness possible for MEMS fabrication. Based on this discussion, we added and revised some sentences as follows:

Research Sentences in Research details (Page. 5)

"…Quartz wafer is widely used as a substrate for micro-nano fabrication due to its visible transparency. …"

Revised and Added Sentences in Research details (Page. 5)

"…Thus, we chose ITO as a total reflector which consumes large area at the bottom of MDM structure. The thickness of ITO is 400 nm, which reduces the electrical resistivity as much as possible to maintain the visible transparency. In case of metal disks, based on the circuit analysis, the lower equivalent impedance is important to maintain the selective emission even though the ITO reflector is used. When the blocked area ratio is small enough to penetrate the visible light, it is possible to maintain the visible transparency. It means that Au as metal disks can be used for decreasing the equivalent impedance. The thickness of Au metal disk is 100 nm with an adhesive layer (Ti) of 10 nm. Ti is a layer for improved adhesion on Si3N4, and does not affect the EM behavior, as shown in the previous work [8]. The pitch is 3 μm, a disk diameter of 0.89 μm. As a dielectric layer, Si3N4 with a thickness of 100 nm is chosen because it has transparency and high permittivity in IR regime, similar to ZnS, which is widely used for IR camouflage material.…."

(Comment #4)

What is the reason to choose Si_3N_4 as the dielectric layer?

(Answer)

The reviewer commented on the choosing reason of Si_3N_4 as the dielectric layer. In general, the MDM structure for IR regime is a transparent material as the dielectric layer such as Al_2O_3 and ZnS. However, these materials are limited in conventional micro-fabrication facilities. Therefore, we change our strategy to use silicon-based materials such as SiO_2 or Si_3N_4 as a dielectric layer. In the case of SiO2, this is quite famous for treating the passivation layer in the microfabrication. However, the relative permittivity is too low to lead to the selective emission. In addition, at 10 μm, the strong lattice resonance induces high emissivity, which is not suitable for our strategy. In the case of Si_3N_4, it has a similar permittivity (5.43 at 5 μm) to ZnS (5.02 at 5 μm). This permittivity can lead to a thin film with a thickness of 100 nm. In general, due to the Beer-Lambert law, all material can be transparent with a thin layer. To check this behavior, we calculate the transmissivity considered by the internal reflection. Figure R2 shows the transmissivity of Si_3N_4 with the wavelength in 3-14 μm.

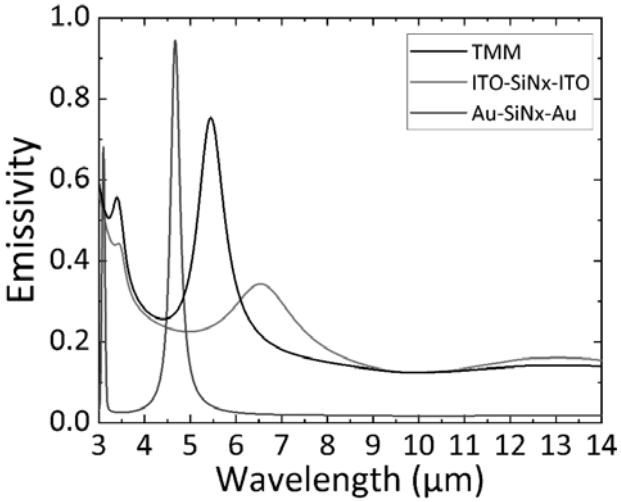

Figure R1. Spectral emissivity of metal-dielectric-metal structure depending on the material in metal parts.

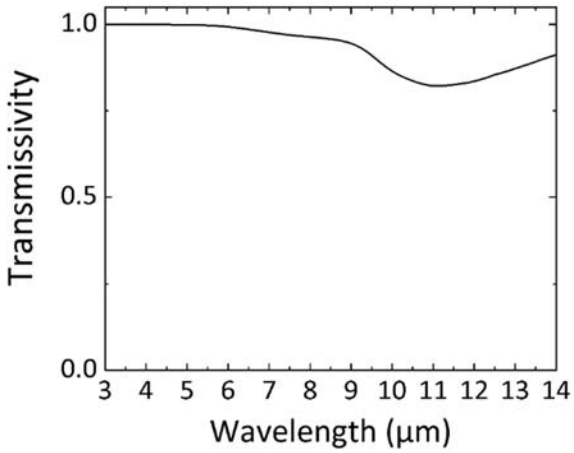

Figure R2. Calculated transmittivity of Si_3N_4 with the thickness of 100 nm used in this study.

As shown in Fig. R2, we understand that the transmissivity is high (> 0.8) except around 10 μm, which is caused by the lattice resonance interacting with the electromagnetic wave. If Si_3N_4 affects the spectral emissivity dominantly, then the peak occurs around 10 μm as decreasing the transmissivity in Fig. R2. In Fig. R1, there is no peak around 10 μm. This result means that the Si_3N_4 has little impact on the spectral emissivity of TMM. These results show that Si_3N_4 can also use the dielectric layer in MDM structure for IR camouflage.

Added Sentences in Research details (Page. 6)

"*As a dielectric layer, Si_3N_4 with a thickness of 100 nm is chosen because it has transparency and high permittivity in IR regime, similar to ZnS, which is widely used for IR camouflage material.*"

(Comment #5)

According to the mechanism of the MIM structure, is there any possibility to replace the top pattern from gold to ITO?

(Answer)

The reviewer asked about the possibility of replacing the top pattern from gold to ITO. To consider the material effect on the spectral emissivity, we simulate MDM structure depending on the material such as indium tin oxide (ITO) and Au. Figure R1 shows the spectral emissivity depending on the material in metal parts.

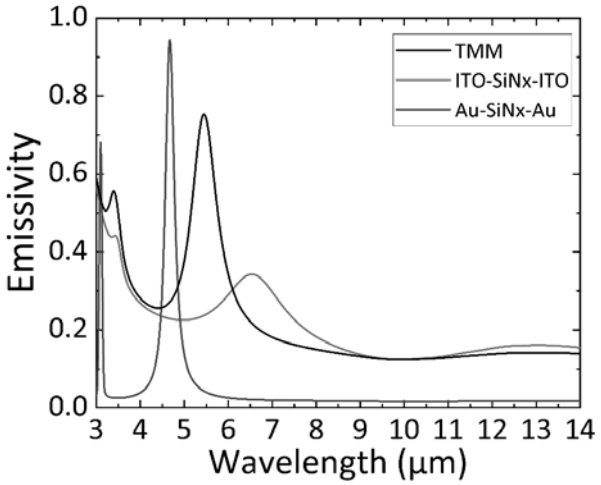

Figure R1. Spectral emissivity of metal-dielectric-metal structure depending on the material in metal parts.

As shown in Fig. R1, we understand the difference in spectral emissivity depending on the material. In the case of Au as metal parts, the emissivity in detected bands is low enough to hide the target, similar to the previous study. Conversely, In the case of ITO as metal parts, the emissivity in detected bands is 0.2, which value is similar to TMM suggested in this study. Generally, the emissivity is related to the electrical conductivity of the material at a certain wavelength. The reason is that particles causing the electrical current interact with the electromagnetic wave and induce the material's reflectivity. Thus, we recognize that only ITO as metal parts in MDM structure cannot be realized for a selective emission sufficiently for IR camouflage.